Mechano-Fenton–Piranha Oxidation of Carbon Nanotubes for Energy Application

Chaohui Wei, Bamidele Akinwolemiwa, Qingfu Wang, Li Guan, Lan Xia, Di Hu, Bencan Tang, Linpo Yu, and George Z. Chen

International Doctoral Innovation Centre, Faculty of Science and Engineering, University of Nottingham Ningbo China, Ningbo, 315100, China
Department of Chemical and Environmental Engineering, Faculty of Science and Engineering, and Key Laboratory of More Electric Aircraft Technology of Zhejiang Province, University of Nottingham Ningbo China, Ningbo, 315100, China

First published 2019

University of Nottingham
UK | CHINA | MALAYSIA

Mechano-Fenton–Piranha Oxidation of Carbon Nanotubes for Energy Application

Chaohui Wei, Bamidele Akinwolemiwa, Qingfu Wang, Li Guan, Lan Xia, Di Hu, Bencan Tang, Linpo Yu, and George Z. Chen**

Emission of nitrogen oxides (NO_x) from chemical processing of materials is a serious environmental concern, frustrating the development of many innovative technologies. For example, sulfonitric oxidation is the most widely used method for processing carbon nanotubes (CNTs), producing a large amount of NO_x. As a result, large scale applications of CNTs for downstream purposes remain challenging. Herein, a NO_x-free oxidation method is proposed for CNTs processing. It starts with mechanically grinding, and then oxidizing the CNTs by hydroxyl radicals in sealed reactors. Such processed CNTs are shorter, possess balanced surface oxygen containing groups without compromising the original CNT integrity, and can disperse readily in water. These are desirable for making various CNT composites, including those with conducting polymers for supercapacitors. The reactors in the process are industrially adoptable, promising a great technological and commercial future.

Photochemical smog, a secondary pollution to air formed by nitrogen oxides (NO_x) reacting with airborne particulates, catalyzed by sunlight, can irritate eyes, throats, and lungs of humans and cause other related diseases, and transportation risk.[1a–c] Of course, NO_x has other detrimental environmental and ecological impacts such as greenhouse effect and acid rain (which causes acidification of soil/ water, plants withering, and corrosion to buildings).[2a,b] The fact is that NO_x exists in a minimum amount in nature, but mostly resulting from anthropogenic activities.[3a,b] Hence, NO_x emission is under stringent regulation and a massive effort has been put for NO_x abatement worldwide.[3b] Current NO_x removal technologies include selective catalytic reduction, wet scrubbing, adsorption, electron beam, electrocatalytic, and bioprocessing.[4a–d] However, their large-scale applications are hindered either by the high cost and energy consumption of the process, or the substandard removal efficiency.[4a–d] This frustration retards many new materials and related technologies from contributing to wealth growth.

A good example is carbon nanotubes (CNTs) which were discovered as early as mid 1980s[5a] and had promised many mate-rial and technological innovations.[5b–d] Unfortunately, these have not happened, largely because of NO_x (see more details below). Interestingly, both CNTs and graphenes are popular for many applications, particularly electrochemical energy storage (EES) devices, such as supercapacitors.[5c,d] Graphenes might exhibit higher specific capacitance in a small quantity,[6a,b] but cannot provide effective electronic and ionic conduction when building devices with a big mass.[6c] On the contrary, CNTs hold a greater advantage for EES devices. They are comparable with graphenes in many aspects,[5c] but would not pack densely as graphenes. Instead, they always offer a porous packing structure that is needed for ion conduction.[6c]

However, commercially available CNTs are highly curved because of defects, and have large aspect ratios and high surface energy.[5b,7a,b] As a result, they can easily tangle together but hardly suspend stably in water. Additionally, their inactive surfaces discourage interactions with other materials when CNTs are adopted as the doping or structural components in various EES materials (composites in most cases).[5c,d,7c] Several methods have been proposed to tackle these issues. For example, surfactants and polymers were used to help CNTs to suspend in water,[8a,b] but could not help interactions between the CNTs and other active components.[8c] Covalent functionalization can modify the properties of CNTs effectively through various reactions, such as oxidation, nitrogenation, sulfonation, cycloaddition, and halogenation,[7d,8d] among which oxidation is the most important method. The CNTs functionalized with oxygen containing

C. Wei, B. Akinwolemiwa
International Doctoral Innovation Centre
Faculty of Science and Engineering
University of Nottingham Ningbo China
Ningbo 315100, P. R. China

Q. Wang, Dr. L. Xia, Dr. D. Hu, Dr. B. Tang, Dr. L. Yu, Prof. G. Z. Chen
Department of Chemical and Environmental Engineering
Faculty of Science and Engineering
and Key Laboratory of More Electric Aircraft Technology of Zhejiang Province
University of Nottingham Ningbo China
Ningbo 315100, P. R. China
E-mail: Linpo.Yu@nottingham.edu.cn

Dr. L. Guan, Prof. G. Z. Chen
Department of Chemical and Environmental Engineering
Faculty of Engineering
University of Nottingham
Nottingham NG7 2RD, UK
E-mail: George.Chen@nottingham.ac.uk

The ORCID identification number(s) for the author(s) of this article can be found under https://doi.org/10.1002/adsu.201900065.

DOI: 10.1002/adsu.201900065

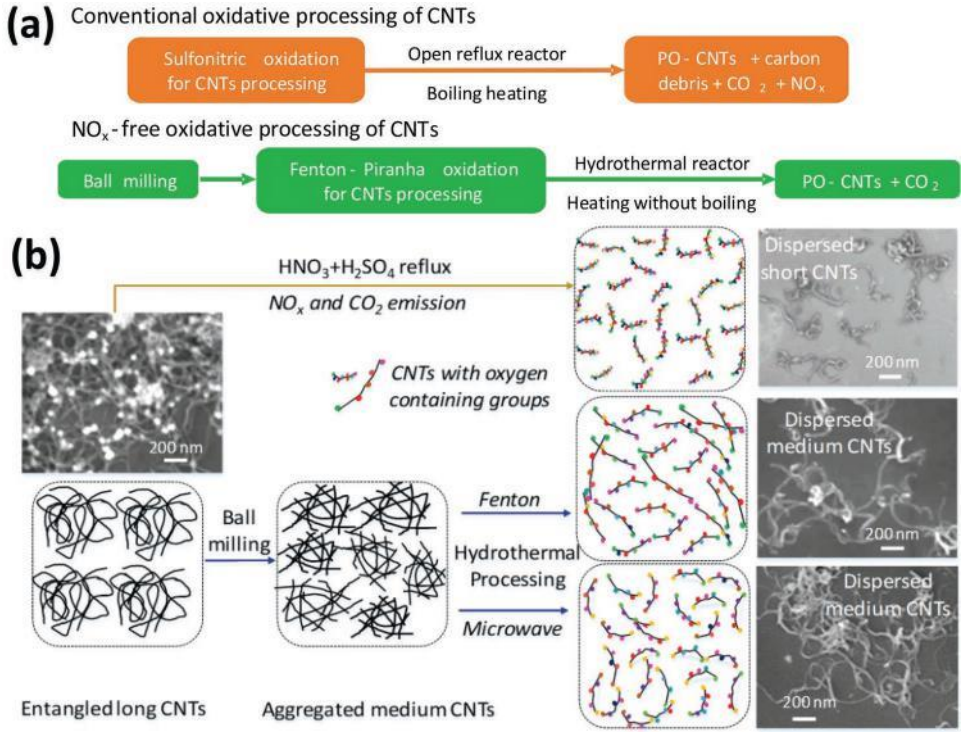

Scheme 1. a) Flow charts of procedures of conventional and NO_x-free processes used in this work. b) SEM images of (clockwise) pristine CNTs, CT-CNTs, BMW-CNTs, and BFHT-CNTs, and schematic illustration of changes of the CNTs following different oxidative processing routes to CT-CNTs, BMW-CNTs, and BFHT-CNTs.

groups (OCGs) can also act as the precursors for other covalent functionalizations.[8e] There are many approaches to oxidize CNTs, involving wet chemical methods,[7d,8d,e] photo-oxidation,[5c,9a] and gas phase treatment.[9b] For example, gas phase oxidation by ozone is a dry and simple process to increase the hydrophi-licity of single walled CNTs.[9c,d] A more popular and widely used bench-scale method is to partially oxidize multiwall CNTs by sul-fonitric acid (mixed concentrated H_2SO_4 and HNO_3) to encourage surface functionalization with various OCGs, and suspension in water.[5c,7a,9e] However, sulfonitric treatments always emit a large amount of NO_x fumes as exemplified in Figure S1a in the Supporting Information. Consequently, there is still no industrial use of this method for oxidative processing of CNTs. Furthermore, the extent of the sulfonitric treatment must be carefully controlled to avoid overoxidation of the CNTs that can lead to a low yield and structural damage.[9e] Thus, it is highly desirable to develop a NO_x-free, less structure damaging, and upscalable process for CNT oxidation to realize those material innovations promised more than three decades ago.

The Piranha solution (PS) is a mixture of H_2SO_4 and H_2O_2 (3:1 to 7:1 v/v) (v for volume), and can oxidize various carbonaceous substances such as CNTs.[9f,g] Piranha oxidation is NO_x-free while the unused H_2SO_4 can be recycled.[10a,b] Reactions (Rcts) (1) and (2) are naturally occurring in the PS.[11a–c] Normally, Rct (1) is more dominant, but Rct (2) determines the power of Piranha oxidation. Although $HO^\bullet$ has a high oxidizing potential (2.8 V vs standard hydrogen electrode),[11c,12a] Piranha oxidation of CNTs was actually found not as strong as sulfonitric oxidation.[5c,7a] One of the reasons is that $HO^\bullet$ has a lifetime of only few nanoseconds in water, and hence may perish before reaching the surface of entangled CNTs[12b–d]

$$H_2O_2 \rightleftharpoons H_2O + 0.5O_2 \quad (1)$$

$$H_2O_2 \rightleftharpoons 2HO^\bullet \quad (2)$$

Herein, we propose a new and NO_x-free oxidative process to achieve partially oxidized CNTs (PO-CNTs) with sub-stantial OCGs (**Scheme 1**a). The process consists of initial mechanical breakage (ball milling (BM)) of the long and entangled CNTs, and then Piranha oxidation in a sealed reactor under mild heating, helping increase the $HO^\bullet$ amount in the PS with or without Fenton's reagent. Such an oxidative process is referred to as mechano-Fenton–Piranha oxidation in the work. The as-produced PO-CNTs in this work behaved highly satisfactorily in composites of polypyrrole/ CNTs (PPy/CNTs) for supercapacitors according to the well-established methods of assessment.[13a,b] All the oxidized CNTs are regarded as PO-CNTs. For convenience, the abbre-viations denoting the CNTs treated by different processes are tabulated in **Table 1**, where a process will be ticked if it was used in the treatment of the corresponding PO-CNTs. The abbreviations of PO-CNTs are further explained in the foot-notes of Table 1.

Ball milling can break CNTs to create more tube-ends and other defects which are both more likely oxidized.[7a,14a,b] In this work, wet ball milling was adopted as the first step to increase the hydrophilicity of the CNT surface,[18a] shorten

Table 1. Summary of the treated CNTs with relevant process details.

		Oxidant			Reactor[a)]		
Abbreviations	BM	Sulfonitric acid	Piranha solution	Fenton–Piranha solution	A	B	C
CT-CNTs		√			√		
BM-CNTs	√						
MWD-CNTs			√			√	
BMW-CNTs	√		√			√	
HT-CNTs			√				√
BHT-CNTs	√		√				√
FHT-CNTs				√			√
BFHT-CNTs	√			√			√

[a)]Reactors A, B, and C correspond to an open reactor (Figure S1a, Supporting Information), a microwave digester (Figure S1b, Supporting Information), and a hydro-thermal reactor (Figure S1c, Supporting Information), respectively. BM is ball milling. 1) CT-CNTs: CNTs from conventional treatment of sulfonitric oxidation, 2) BM-CNTs: CNTs grounded by ball milling, 3) MWD-CNTs: CNTs treated by Piranha solution in a microwave digester, 4) BMW-CNTs: Piranha oxidation of BM-CNTs in a microwave digester, 5) HT-CNTs: CNTs treated by Piranha solution in a hydrothermal reactor, 6) BHT-CNTs: BM-CNTs treated by Piranha solution in a hydrothermal reactor, 7) FHT-CNTs: CNTs treated by Fenton–Piranha oxidation in a hydrothermal reactor, and 8) BFHT-CNTs: obtained from ball milling and Piranha–Fenton oxidation in a hydrothermal reactor. All the oxidized CNTs are regarded as PO-CNTs.

the length of CNTs, and decrease the size of the CNT agglomerates.[14a,b] The cluster size of BM-CNTs was found to decrease with an increase of the milling speed (**Figure 1**a). More details for optimal ball milling are given in Figures S2 and S3 in the Supporting Information, confirming that higher speed milling could produce shorter CNTs in smaller clusters. Then, Fenton's reagent was used to accelerate the generation of HO• and other radicals according to Rcts (3) and (4).[9b,15] A sealed reactor can also help increase the amount of HO• by depressing the oxygen gas generation as described in Rct (1), leading to a favor on Rct (2) according to Le Chat-elier's principle.[16a] The sealed reactor can be either an oil-bath heated hydrothermal reactor[11a,16b] or a microwave digester[16c] under a quasi-hydrothermal condition

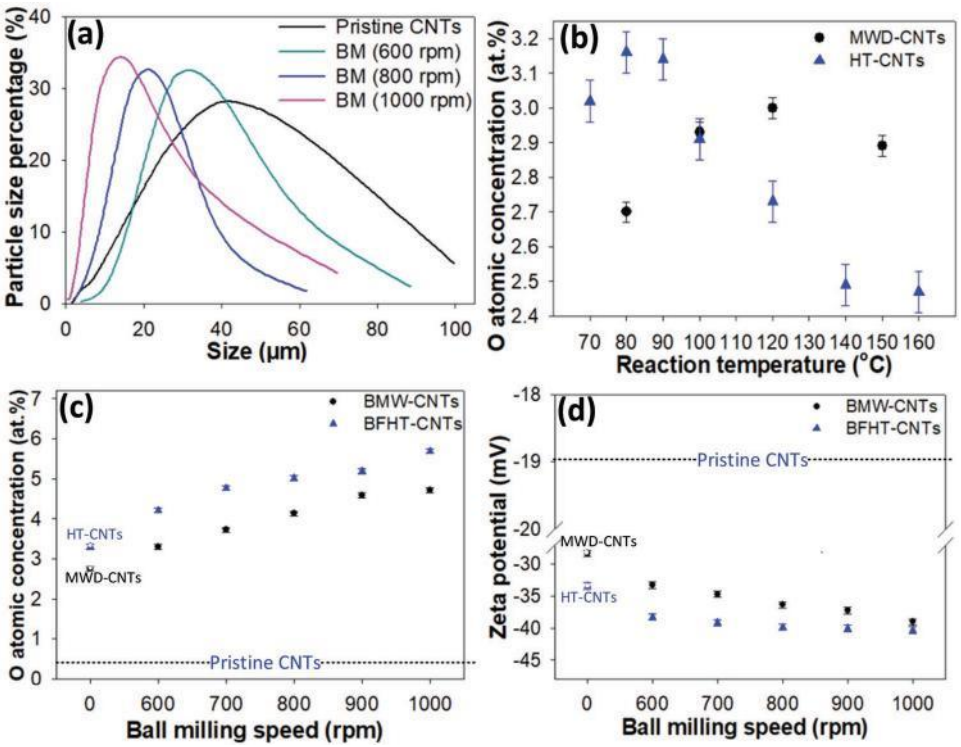

Figure 1. a) Particles size distribution of CNTs milled under different rotation speeds. b) Oxygen atomic concentration of MWD-CNTs and HT-CNTs at different reaction temperatures. c) OAC of pristine CNTs, BMW-CNTs, and BFHT-CNTs at ball milling speed from 600–1000 rpm. MWD-CNTs were obtained at a reaction temperature of 120 °C and reaction time of 3 h. HT-CNTs were obtained at a reaction temperature of 80 °C and reaction time of 3 h. d) Zeta potentials of pristine CNTs, BMW-CNTs, and BFHT-CNTs at ball milling speed from 600–1000 rpm.

$$Fe^{2+} + H_2O_2 + H^+ \rightarrow Fe^{3+} + H_2O + HO^{\bullet} \quad (3)$$

$$Fe^{3+} + H_2O_2 \rightarrow Fe^{2+} + HOO^{\bullet} + H^+ \quad (4)$$

A series of Piranha oxidation experiments were conducted in a microwave digester and hydrothermal reactor at different temperature for different reaction time. The optimized reaction temperature for MWD-CNTs and BHT-CNTs are 120 and 80 °C, respectively (Figure 1b). The oxygen atomic concentrations (OACs) and zeta potentials of CNTs versus ball milling speed are shown in Figure 1c,d, respectively. The relevant data of pristine CNTs and MWD/HT-CNTs are also presented as dashed lines and hollow symbols, respectively, in both Figure 1c,d. BMW-CNTs possess higher OAC compared with MWD-CNTs (Figure 1c), indicating that BM-CNTs are more favorable for the oxidative process than pristine CNTs due to the substantial reactive sites in BM-CNTs such as tube-ends and defects.[7a,14a,b] Additionally, the smaller CNT clusters size can help to reduce the transportation time for $HO^{\bullet}$ to approach CNT surfaces and thus more CNTs can react with $^{HO\bullet}$.[14a,15] The OAC of BMW-CNTs increases with increase in rotation speed (Figure 1c). Hereby, a high milling speed is advantageous for introducing OCGs in CNTs. The effect of Fenton's reagent was investigated by oxidizing CNTs in a hydrothermal reactor with different oxidants. The OAC of BHT-CNTs exhibits a roughly 30% increase compared with that of HT-CNTs (Figure S8, Supporting Information), which can be explained by the same reason for the OAC increase of BMW-CNTs. There was a 10% rise in the OAC of PO-CNTs when the Piranha solution (producing HT-CNTs) was replaced by Fenton–Piranha solution (producing FHT-CNTs) in a hydrothermal reactor (Figure S8, Supporting Information). Such rise can be attributed to the catalytic effect of Fe^{2+} triggering the continuous production of $HO^{\bullet}$ in the reaction solution for CNTs oxidation.[9b,15] Due to the synergic drives from ball milling and Fenton reaction in the oxidative process of CNTs, the OAC of BFHT-CNTs is higher than that of HT-CNTs. Moreover, the OAC of BFHT-CNTs increases with increase in milling speed (Figure 1c).

Zeta potential represents the electrostatic interaction between colloidal particles which determines the colloidal stabilities of suspensions.[8a,9e] Zeta potentials of BMW-CNTs are more negative than that of MWD-CNTs (Figure 1d). Moreover, the zeta potentials of BMW-CNTs are proportional to the milling speed indicating that BM-CNTs are more advantageous to introducing OCGs in CNT surfaces. These OCGs can reduce the hydrophobicity of CNTs and enhance the stability of CNT suspensions.[8a,9e] The zeta potentials of BFHT-CNTs are more negative than that of BHT-CNTs or FHT-CNTs (Figure S8, Supporting Information) due to the same reason as discussed for Figure 1c. Also, the zeta potential of BFHT-CNTs increases in the negative direction with increase in rotation speed of ball milling and they are in the range of □35 to □45 mV. It means BFHT-CNTs can suspend in water moderatly.[18c] More details for the explanation of Fenton reaction and optimization of the reaction temperature and time for CNTs oxidation in these two sealed reactors can be found in Figures S4–S10 in the Supporting Information. It was observed that higher milling speed and Fenton's reagent helped produce CNTs with more OCGs from the data analysis of thermogravimetric analysis (TGA), X-ray photoelectron spectroscopy (XPS), Raman spectroscopy, and zeta potential. For instance, Raman spectroscopy revealed that the edge defects of CNTs increased with the ball milling speed (see Figures S3b, S5b, and S10b in the Supporting Information). Thus, the OCGs can be more effectively functionalized on the ball milled CNTs than the ones without ball milling.

Scanning electron microscopic (SEM) images of the pristine CNTs, CT-CNTs, BMW-CNTs, and BFHT-CNTs are presented in Scheme 1b, respectively. The samples were prepared by dropping 10 ∝L of the CNT suspension of 40 mg L□¹ on a silicon wafer. Scheme 1b shows on the left side a typical agglomerate of hundreds of entangled CNTs with an average diameter over 1 ∝m, which is too large for stable suspension in water. CT-CNTs could stably suspend in water and had the shortest length leading to the smallest agglomerate among all the CNT samples in Scheme 1b. Some tiny fragments can be seen in the top-right image of Scheme 1b due to the strong sulfonitric oxidation. Both BMW-CNTs and BFHT-CNTs were shorter than pristine CNTs, but longer than CT-CNTs (Scheme 1b). The TEM images of the four CNTs are shown and described in Figure S11 in the Supporting Information. The structural integrity of PO-CNTs was also confirmed by the thermogravimetric analysis as shown in Figure S12a in the Supporting Information. The weight losses of BFHT-CNTs and BMW-CNTs are much smaller than the one of CT-CNTs at the same temperature in TGA, revealing that BFHT-CNTs and BMW-CNTs have greater thermal stability than CT-CNTs. This is because less OCGs in the structure of BMW-CNTs and BFHT-CNTs after the oxidation cause less damages. Such properties were transmitted to the respective PPy/PO-CNTs composites as shown in Figure S12b in the Supporting Information.

The suspensions of both BMW-CNTs and BFHT-CNTs are more stable than the pristine CNTs, also suggesting that the surfaces of BMW-CNTs and BFHT-CNTs have more OCGs. Photographs of the BMW-CNT and BFHT-CNT suspensions that stood still for over 20 days can be found in Figure S13 in the Supporting Information. The suspension stability of the pristine CNTs and PO-CNTs are also further confirmed by UV–vis in Figure S14 in the Supporting Information. It should be noted that the yields of BMW-CNTs and BFHT-CNTs were as high as 80–95%. In contrast the yield of CT-CNTs was only 40–65%.

X-ray photoelectron spectroscopy was applied to study the elemental constitution and chemical bonding of functional-ized CNTs.[7a,9e,17a] The spectra of the pristine CNTs, CT-CNTs, BMW-CNTs, and BFHT-CNTs are shown in **Figure 2**a, while the deconvolutions of the XPS O1s of CT-CNTs, BMW-CNTs, and BFHT-CNTs are interpreted in Figure 2b–d, respectively. XPS C1s shows a peak at 284.5 eV (in pink circles) and O1s at 532.0 eV (in purple circles) in **Figure** ^{3a}.[17a,b] The peak heights can correlate to the elemental contents.[17a,b] The calculated content of oxygen in pristine CNTs, CT-CNTs, BMW-CNTs, and BFHT-CNTs were 0.33, 11.26, 4.72, and 5.69 at%, respectively. The oxygen content in CT-CNTs was markedly higher than that in BMW-CNTs and BFHT-CNTs, indicating a larger amount of OCGs in the surface of CT-CNTs than that of the other two PO-CNTs.

Deconvolutions of XPS O1s for different PO-CNTs showed the existence of two main types of OCGs. The peaks at 532.2–532.54 eV can be attributed to carbonyl groups (C=O), while

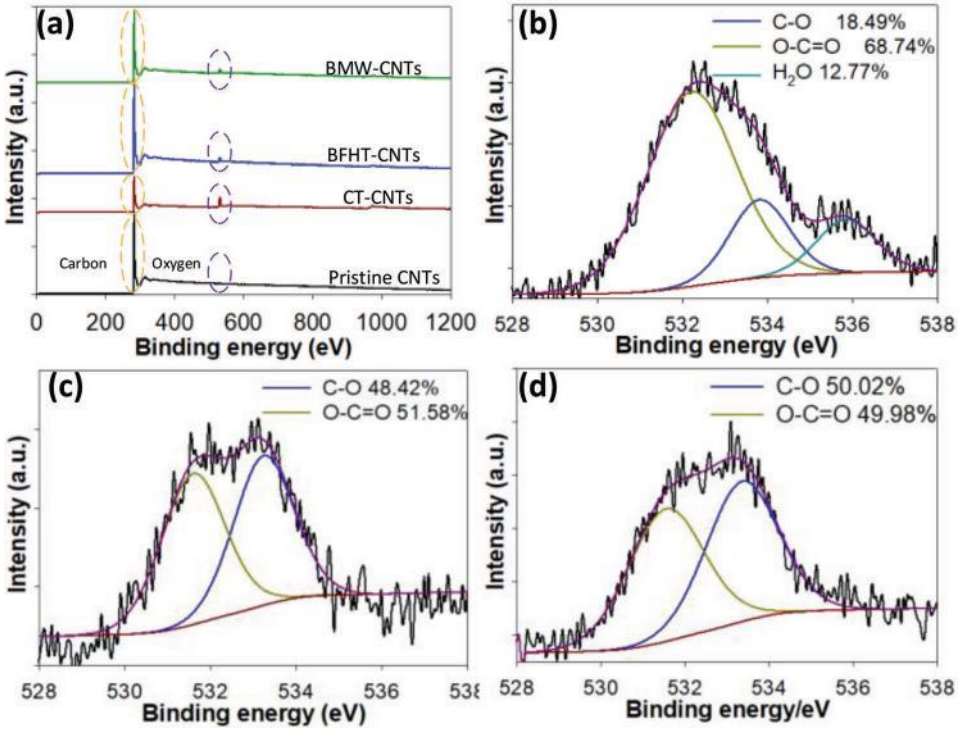

Figure 2. a) XPS spectra of the pristine CNTs, CT-CNTs, BFHT-CNTs, and BMW-CNTs. Deconvolutions of the XPS O1s of b) CT-CNTs, c) BMW-CNTs, and d) BFHT-CNTs.

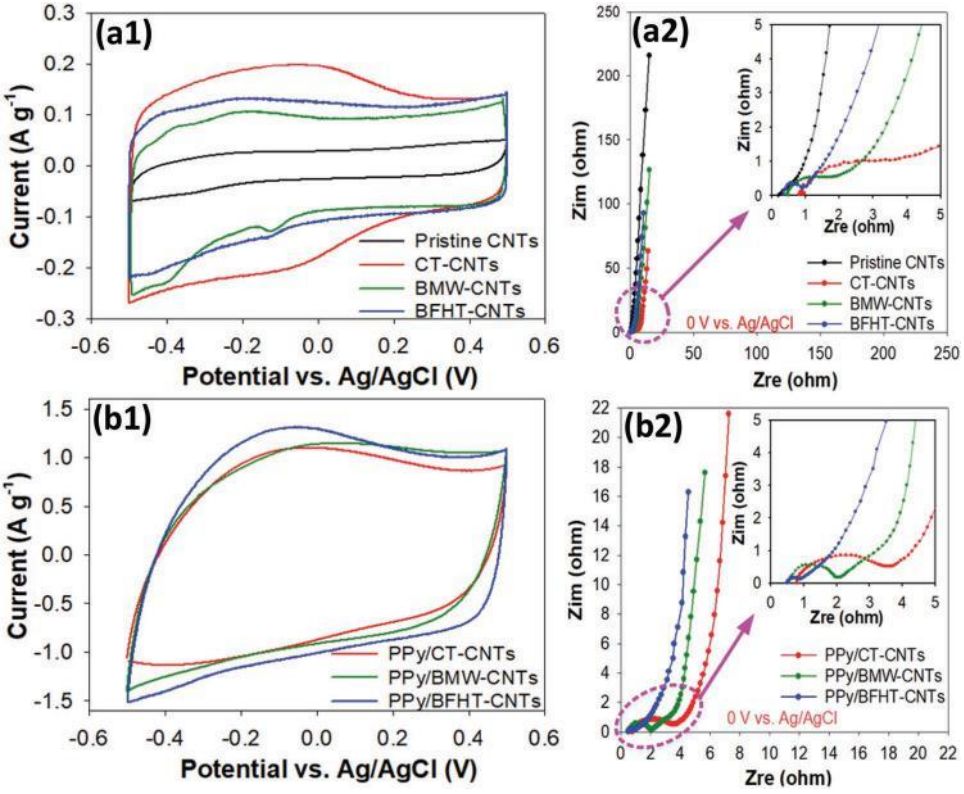

Figure 3. Cyclic voltammograms (CVs) of the different a1) CNTs and b1) PPy/PO-CNTs composites with 5 wt% of polytetrafluoroethylene (PTFE) binder in the potential range of −0.5 to 0.5 V versus Ag/AgCl at a scan rate of 5 mV s^{-1} in 3 mol L^{-1} KCl electrolyte. The counter electrode was a graphite rod. Nyquist plots of the different a2) CNTs and b2) PPy/CNTs composites at 0 V versus Ag/AgCl. Inset: A zoomed view is indicated.

the peaks at 533.3–533.8 eV to the carbon-oxygen singe bond (C–O).[9e,17a,b] From Figure 2b, it can be seen that the majority of OCGs in CT-CNTs were C=O groups, whiles the OCGs in BMW-CNTs and BFHT-CNTs consisted of both C–O and C=O groups. The deconvolutions of C1s of pristine CNTs and PO-CNTs are in consistency with the results of O1s deconvolu-tion (Figure S15, Supporting Information). The temperature programmed desorption (TPD) results of the CNT samples can support the discussions above (Figure S16, Supporting Information) and provide more details in OCGs on the CNTs. It suggests that sulfonitric oxidation modified the CNTs with more OCGs at higher oxidation states (68.74% of C=O groups).

In contrast, the CNTs treated by the PS alone in an open refluxing reactor achieved a low oxygen content of 2.35 at% of which only 11.32% were C=O (Figure S17, Supporting Information). It could be that, when HO• attacked the CNTs, C–O was produced (Schemes S1–S3, Supporting Information). Further oxidation from C–O to C=O would require additional oxidants on site, but HO• has a short life in water and also undersupply due to Rct (1). C=O may also form directly if HO• reacted with the defects which were however rare in pristine CNTs.

It should be mentioned that there are always iron impurities in both the as-received CNTs (CNT: 98 wt%) and PO-CNTs treated by the mechano-Fenton–Piranha oxidation. However, an enlarged view of Figure 2a is shown in Figure S17c in the Supporting Information indicating that there is no iron or its compounds on the surface or outer layers of these CNT samples. It is reasonable to assume that the iron impurity should be located inside the tubes and the integrity of these PO-CNTs makes it difficult to wash this iron impurity away by acid. It is known that soluble redox impurity like iron (II and III) has a shuttle effect to minimize the energy capacity of the electrode materials. It is essential to wash away all the iron impurity from the CNT samples by acid. In our case, the main iron impurity was inside the CNTs and had very low possibility to contact with the electrolyte when the CNTs were used as the electrode materials. The other iron impurity outside the CNTs was washed away during the washing process as described in the Supporting Information.

Upon ball milling, shorter CNTs in smaller agglomerates were produced with newly generated defects. In the sealed reactor, the supply of HO• was also increased. As a result, C–O could be further oxidized into C=O (Scheme S4, Supporting Information). Hence, there were higher contents of oxygen and greater percentages of C=O in both BMW-CNTs and BFHT-CNTs.

Different CNT oxidation processes are compared, showing that the sulfonitric treatment involves massive NO_x emission which is absent in Piranha oxidation (Scheme 1a). Sulfonitric oxidation of CNTs can be violent, producing a greater amount of OCGs in CNTs surfaces and cutting down the pristine CNTs into shorter tubes and fragments (Scheme 1b), which also schematically presents the intermediate and final products of ball milling and Piranha oxidation processes. It is very important that ball milling made CNTs shorter in smaller aggregates with added defects. These changes make it easy for the reaction with HO•. It can be concluded that BMW-CNTs are averagely shorter than BFHT-CNTs based on the UV–vis results (Figure S14, Supporting Information).

Although BMW-CNTs and BFHT-CNTs possessed less OCGs than CT-CNTs, the former suspended in water with sufficient stability for the synthesis of PPy/CNT composites which were then assessed for capacitive charge (energy) storage.[13a,b,17c] Cyclic voltammograms (CVs) of the different CNTs in between −0.5 and 0.5 V versus Ag/AgCl at 5 mV s^{-1} are shown (Figure 3a1). All these CVs are rectangular, indicating capacitive charging and discharging. As expected from the effect of OCGs, the CVs prove that all PO-CNTs exhibited markedly larger capacitance than the pristine CNTs. The calculated specific capacitance, $_{Csp,}$ agreed with the XPS analysis of the OCG types and contents. A $_{Csp}$ value of 33.0 F g^{-1} was achieved for CT-CNTs, compared to 23.5 F g_{-1} for BMW-CNT, and 24.7 F g_{-1} for BFHT-CNT, because of the different amounts and types of OCGs on the PO-CNT surfaces.[18a,b] The different $_{Csp}$ values can also be explained by the different interruptions of electron delocalization by the OCGs on the CNTs.[6c,18c]

Nyquist plots of electrochemical impedance spectroscopy (EIS) for different CNTs at 0 V versus Ag/AgCl are presented in Figure 3a2. It was found that the knee frequency of CT-CNTs (31.6 Hz) was much lower than BMW-CNTs (316.0 Hz) and BFHT-CNTs (794.3 Hz). Generally, the higher the knee frequency is, the faster the charge transfer rate can [be.][13a,b] The higher knee frequencies of BMW-CNTs and BFHT-CNTs can be ascribed to the better preserved structures in both BMW-CNTs and BFHT-CNTs, retaining the high electronic conductivity of CNTs and hence high charge transfer rate.

CVs of the PPy/CNT composites are shown (Figure 3b1). The calculated $_{Csp}$ values of the PPy/CT-CNT, PPy/BMW-CNT, and PPy/BFHT-CNT composites were 153.2, 166.1, and 192.0 F g^{-1}, respectively. Because the amount of PPy was approximately the same in all the PPy/CNT composites, their $_{Csp}$ values would depend strongly on the electronic conductivity and charge transfer rate. This can be further confirmed by the Nyquist plots in Figure 3b2 where the PPy/CT-CNT has the lowest knee frequency (PPy/CT-CNT: 15.9 Hz, PPy/BMW-CNT: 100.0 Hz, and PPy/BFHT-CNT: 199.5 Hz), and consequently the slowest charge transfer rate in all composites as indicated by the largest semicircle of PPy/CT-CNT. When the knee frequency is considered, the interrelationship among the three composites is in consistence with that among the three PO-CNTs (Figure 3a2,b2), suggesting that the interaction between CNTs and PPy may be greatly affected by the OCGs in the CNT surfaces and reservation of CNT structures. After 1000 CV cycles in the potential range from −0.5 to 0.5 V versus Ag/AgCl, the capacitance retention before and after cycling are 85.7%, 89.3%, and 91.5% for PPy/CT-CNTs, PPy/BMW-CNTs, and PPy/BFHT-CNTs, respectively, as shown in Figure S18 in the Supporting Information. The higher structural integrity of BMW-CNTs and BFHT-CNTs are inherited to the corresponding PPy/PO-CNTs composite so the composite can resist the stress and fatigue due to repeated intercalation and depletion of ions during cycling.

In summary, we have proposed an environment-friendly (i.e., NO_x-free) mechano-hydrothermal process to efficiently oxidize CNTs without damaging changes in structure. In the new process, the initial ball milling produces shorter and more end-and surface-defected CNTs in smaller agglomerates, which can facilitate the oxidation by HO• and produce CNTs with balanced amounts and types of OCGs in the follow-on Piranha–Fenton oxidation. It has been shown that sealing and mild heating the oxidation reactor, which resembles a quasi-hydrothermal condition, can maintain a sufficient supply of HO• by avoiding

decomposition of H_2O_2 into water and the oxygen gas. Such produced CNTs remain highly electronically conducting and suspend well in water. They can form composites with polypyrrole effectively for capacitive charge storage. Moreover, our new method should be industrially adaptable, offering a NO_x-free replacement for the widely used sulfonitric oxidation method for CNT processing with a particular promise for making various CNT-based energy storage materials at large scales.

Supporting Information

Supporting Information is available from the Wiley Online Library or from the author.

Acknowledgements

This work received funding from the International Doctoral Innovation Centre, Ningbo Education Bureau, Ningbo Science and Technology Bureau, University of Nottingham, Ningbo Municipal Bureau of Science and Technology (3315 Plan and 2014A35001-1), Natural Science Foundation of Zhejiang Province (2017C31104 and LY19B030004), and UK Engineering and Physical Sciences Research Council (EP/J000582/1 and GR/R68078).

Conflict of Interest

The authors declare no conflict of interest.

Keywords

ball milling, carbon nanotube, Fenton's reagent, oxidation, Piranha solution

Received: June 3, 2019
Revised: July 17, 2019
Published online:

[1] a) L. Xue, R. Gu, T. Wang, X. Wang, S. Saunders, D. Blake, P. K. Louie, C. W. Luk, I. Simpson, Z. Xu, I. Gavriil, *Atmos. Chem. Phys.* **2016**, *16*, 9891; b) A. Chaloulakou, I. Mavroidis, *Atmos. En'iron.* **2008**, *42*, 454; c) B. Rani, U. Singh, A. Chuhan, D. Sharma, R. Maheshwari, *J. Ad'. Sci. Res.* **2011**, *2*, 28.

[2] a) W. Winiwarter, Z. Klimont, *Curr. Opin. En'iron. Sustainability* **2011**, *3*, 438; b) J. Dora, M. A. Gostomczyk, M. Jakubiak, W. Kordylewski, W. Mista, M. Tkaczuk, *Chem. Process Eng.* **2009**, *30*, 621.

[3] a) F. Liu, S. Beirle, Q. Zhang, B. Zheng, D. Tong, K. He, *Atmos. Chem. Phys.* **2017**, *17*, 9261; b) B. N. Duncan, L. N. Lamsal, A. M. Thompson, Y. Yoshida, Z. Lu, D. G. Streets, M. M. Hurwitz, K. E. Pickering, *J. Geophys. Res.: Atmos.* **2016**, *121*, 976.

[4] a) Y. Sun, E. Zwolin´ska, A. G. Chmielewski, *Crit. Re'. En'iron. Sci. Technol.* **2016**, *46*, 119; b) K. Skalska, J. S. Miller, S. Ledakowicz, *Sci. Total En'iron.* **2010**, *408*, 3976; c) H. W. Yen, S. H. Ho, C. Y. Chen, J. S. Chang, *Biotechnol. J.* **2015**, *10*, 829; d) L. Guo, Y. Shu, J. Gao, *Energy Procedia* **2012**, *17*, 397.

[5] a) H. G. Tennent, *US Patent 4663230*, **1984**; b) D. Tasis, N. Tagmatarchis, A. Bianco, M. Prato, *Chem. Re'.* **2006**, *106*, 1105; c) C. Wei, B. Akinwolemiwa, L. Yu, D. Hu, G. Z. Chen, in *Polymer Composites with Functionalized Nanoparticles* (Eds: K. Pielichowski, T. M. Majka), Elsevier, New York **2019**, pp. 211–248; d) M. Noked, S. Okashy, T. Zimrin, D. Aurbach, *Angew. Chem., Int. Ed.* **2012**, *51*, 1568.

[6] a) S. Chen, J. Zhu, X. Wu, Q. Han, X. Wang, *ACS Nano* **2010**, *4*, 2822; b) X. Jin, W. Zhou, S. Zhang, G. Z. Chen, *Small* **2007**, *3*, 1513; c) G. Z. Chen, *Prog. Nat. Sci.: Mater. Int.* **2013**, *23*, 245.

[7] a) V. Datsyuk, M. Kalyva, K. Papagelis, J. Parthenios, D. Tasis, A. Siokou, I. Kallitsis, C. Galiotis, *Carbon* **2008**, *46*, 833; b) M. Holzinger, O. Vostrowsky, A. Hirsch, F. Hennrich, M. Kappes, R. Weiss, F. Jellen, *Angew. Chem., Int. Ed.* **2001**, *40*, 4002; c) Z. Syrgiannis, B. Gebhardt, C. Dotzer, F. Hauke, R. Graupner, A. Hirsch, *Angew. Chem., Int. Ed.* **2010**, *49*, 3322; d) K. Balasubramanian, M. Burghard, *Small* **2005**, *1*, 180.

[8] a) B. White, S. Banerjee, S. O'Brien, N. J. Turro, I. P. Herman, *J. Phys. Chem. C* **2007**, *111*, 13684; b) B. Wu, D. Hu, Y. Kuang, B. Liu, X. Zhang, J. Chen, *Angew. Chem.* **2009**, *121*, 4845; c) M. Yoonessi, M. Lebrón-Colón, D. Scheiman, M. A. Meador, *ACS Appl. Mater. Interfaces* **2014**, *6*, 16621; d) U. N. Maiti, W. J. Lee, J. M. Lee, Y. Oh, J. Y. Kim, J. E. Kim, J. Shim, T. H. Han, S. O. Kim, *Ad'. Mater.* **2014**, *26*, 40; e) M. Melchionna, M. Prato, *ECS J. Solid State Sci. Technol.* **2013**, *2*, M3040.

[9] a) M. Lebrón-Colón, M. Meador, D. Lukco, F. Solá, J. Santos-Pérez, L. McCorkle, *Nanotechnology* **2011**, *22*, 455707; b) X. Zhang, L. Lei, B. Xia, Y. Zhang, J. Fu, *Electrochim. Acta* **2009**, *54*, 2810; c) P. P. Pal, T. Larionova, I. V. Anoshkin, H. Jiang, M. Nisula, A. A. Goryunkov, O. V. Tolochko, M. Karppinen, E. I. Kauppinen, A. G. Nasibulin, *J. Phys. Chem. C* **2015**, *119*, 27821; d) J. Simmons, B. Nichols, S. Baker, M. S. Marcus, O. Castellini, C.-S. Lee, R. Hamers, M. Eriksson, *J. Phys. Chem. B* **2006**, *110*, 7113; e) S. Gómez, N. M. Rendtorff, E. F. Aglietti, Y. Sakka, G. Suárez, *Appl. Surf. Sci.* **2016**, *379*, 264; f) K. J. Ziegler, Z. Gu, H. Peng, E. L. Flor, R. H. Hauge, R. E. Smalley, *J. Am. Chem. Soc.* **2005**, *127*, 1541; g) X. Lu, W.-L. Yim, B. H. Suryanto, C. Zhao, *J. Am. Chem. Soc.* **2015**, *137*, 2901.

[10] a) J. Fraga-Dubreuil, K. Bourahla, M. Rahmouni, J. P. Bazureau, J. Hamelin, *Catal. Commun.* **2002**, *3*, 185; b) J. Van Groenestijn, O. Hazewinkel, R. Bakker, *Sugar Ind.* **2006**, *131*, 639.

[11] a) J. R. Portela, J. Lopez, E. Nebot, E. M. de la Ossa, *J. Hazard. Mater.* **2001**, *88*, 95; b) C. P. Huang, C. Dong, Z. Tang, *Waste Manage.* **1993**, *13*, 361; c) G. V. Buxton, C. L. Greenstock, W. P. Helman, A. B. Ross, *J. Phys. Chem. Ref. Data* **1988**, *17*, 513.

[12] a) S. Kommineni, J. Zoeckler, A. Stocking, P. Liang, A. Flores, R. Rodriguez, T. Brown, R. Per, A. Brown, *3.0 Ad'anced Oxidation Processes*, Center for Groundwater Restoration and Protection National Water Research Institute, Los Angeles, CA **2000**, pp. 110–208; b) H. Sies, *Eur. J. Biochem.* **1993**, *215*, 213; c) I. Isaksen, S. Dalsøren, *Science* **2011**, *331*, 38; d) W. Li, Y. Bai, Y. Zhang, M. Sun, R. Cheng, X. Xu, Y. Chen, Y. Mo, *Synth. Met.* **2005**, *155*, 509.

[13] a) G. Z. Chen, M. S. Shaffer, D. Coleby, G. Dixon, W. Zhou, D. J. Fray, A. H. Windle, *Ad'. Mater.* **2000**, *12*, 522, b) C. Peng, J. Jin, G. Z. Chen, *Electrochim. Acta* **2007**, *53*, 525.

[14] a) B. Munkhbayar, M. J. Nine, J. Jeoun, M. Bat-Erdene, H. Chung, H. Jeong, *Powder Technol.* **2013**, *234*, 132; b) S. K. Smart, W. Ren, H. Cheng, G. Lu, D. J. Martin, *Int. J. Nanotechnol.* **2007**, *4*, 618.

[15] C. Fan, W. Li, X. Li, S. Zhao, L. Zhang, Y. Mo, R. Cheng, *Chin. Sci. Bull.* **2007**, *52*, 2054.

[16] a) J. A. Campbell, *J. Chem. Educ.* **1985**, *62*, 231; b) I. Hasegawa, Y. Inoue, Y. Muranaka, T. Yasukawa, K. Mae, *Energy Fuels* **2011**, *25*, 791; c) M. Steimecke, S. Ruemmler, M. Bron, *Electrochim. Acta* **2015**, *163*, 1.

[17] a) T. Okpalugo, P. Papakonstantinou, H. Murphy, J. McLaughlin, N. Brown, *Carbon* **2005**, *43*, 153; b) H. Liu, H. Song, X. Chen, S. Zhang, J. Zhou, Z. Ma, *J. Power Sources* **2015**, *285*, 303.

[18] a) B. Akinwolemiwa, C. Wei, G. Z. Chen, *Electrochim. Acta* **2017**, *247*, 344; b) L. Yu, G. Z. Chen, *J. Power Sources* **2016**, *326*, 604; c) J. Li, J. O'Shea, X. Hou, G. Z. Chen, *Chem. Commun.* **2017**, *53*, 10414.